Journal of the Serbian Chemical Society
JSCS-info@shd.org.rs • www.shd.org.rs/JSCS
J. Serb. Chem. Soc. *88* (2) 141–152 (2023)
JSCS–5616
Original scientific paper
Published 18 November 2022

Dissociation of N_2 by electron impact in electric and magnetic RF fields

MIROSLAV RISTIĆ[1]*[#], RADOMIR RANKOVIĆ[1], MIRJANA M. VOJNOVIĆ[2], VIOLETA V. STANKOVIĆ[2] and GORAN B. POPARIĆ[2]

[1]*University of Belgrade, Faculty of Physical Chemistry, P. O. Box 47, 11000 Belgrade, Serbia and* [2]*University of Belgrade, Faculty of Physics, P. O. Box 44, 11000 Belgrade, Serbia*

(Received 10 July, revised 5 August, accepted 8 August 2022)

Abstract: Rate coefficients for electron impact dissociation of the N_2 molecule under the influence of crossed radio-frequency (RF) electric and magnetic fields were calculated for field frequencies of 13.56, 100 and 200 MHz and for root mean square values of the reduced electric field strength of 300 and 500 Td. The root mean square values of the reduced magnetic field were varied from 0 to 2000 Hx. The effects of the strength of the RF fields and their frequency on the rates for the dissociation to neutral fragments and for the dissociative ionization are discussed. The temporal evolution of the rate coefficients during one period of the RF field is shown and discussed.

Keywords: nitrogen molecule; neutral fragments; dissociative ionization.

INTRODUCTION

In addition to being the main component of the Earth's atmosphere, nitrogen is abundantly present in the atmospheres of Pluto, Titan and Triton, and in smaller quantities on Mars and Venus. Nitrogen is also used in many RF discharge-based technologies, such as nitriding of materials,[1] plasma polymerization,[2] production of nanomaterials,[3] medical sterilizations,[4] doping of graphene and many others.[5] In all these environments, the nitrogen molecules are exposed to collision with electrons. From the aspect of chemical reactivity of nitrogen plasma, one of the most important elementary processes in these collisions is certainly dissociation. Dissociation can occur to form two neutral nitrogen atoms and this reaction is known as the dissociation into neutral fragments:

$$e^- + N_2 \rightarrow N_2^* \rightarrow N + N + e^- \quad (1)$$

* Corresponding author. E-mail: ristic@ffh.bg.ac.rs
# Serbian Chemical Society member.
https://doi.org/10.2298/JSC220710066R

The threshold energy for reaction (1) is 9.75 eV* and the majority of the electronic states of the N_2 molecule lie above this energy. Excess energy during dissociation is transferred to atoms.

Zipf and McLaughlin recognized the importance of dissociation of excited N_2 molecules over radiative relaxation *via* a manifold of singlet valence and Rydberg states.[6] They came to the conclusion that nitrogen molecules that were excited to various $^1\Pi_u$ and $^1\Sigma_u^+$ states, whether by electron impact or UV photon absorption, mostly follow the predissociation path (*i.e.*, the radiationless transition of a molecule from a stable excited state to an unstable excited state that leads to dissociation). Photon relaxations from these singlet states *via* dipole-allowed transitions to the singlet ground state were expected to be dominant,[7] but it turned out that they last much longer than the dissociation. Namely, dissociation to neutrals occurs in a time interval of 10^{-13} s, while photon relaxation lasts 10^{-8} s.[8] The main contribution to reaction (1) for electron energies lower than 100 eV stems from a family of $^1\Pi_u$ states, which predissociate with almost 100 % efficiency. The contributions of $^1\Sigma_u^+$ states to dissociation vary depending on the vibrational level of the state.

At higher values of the electron energy (above 100 eV), the probability increases that the N atom and N^+ are formed during dissociation, instead in reaction of two N atoms. This process can be presented by the following reaction:

$$e^- + N_2 \rightarrow N_2^* \rightarrow N^+ + N + 2e^- \quad (2)$$

and it is called dissociative ionization. It is competitive with reaction (1) and it has a threshold value of 24.29 eV.[9]

In this manuscript, the rate coefficients for the dissociation to neutral fragments and for dissociative ionization, under the presence of crossed RF electric and RF magnetic field, which is a situation that corresponds to the one that exists in inductively coupled plasmas, are presented. The rate coefficients were calculated for values of fields frequencies of 13.56, 100 and 200 MHz and for different strength values of electric and magnetic fields. For this purpose, the electron energy distribution functions (EEDFs) that were obtained by Monte Carlo simulation, and the appropriate cross sections for processes (1) and (2) were used. The integral cross sections for dissociation into neutral fragments that were measured and rescaled by Cosby were adopted.[10] Cosby obtained integral cross section (ICS) by directly detecting the correlated fragment pair N + N, by a time and position sensitive detector.[10] The measured ICS were further adjusted by Cosby according to the results of Winters and as such are generally recommended and used in this work.[11,12] Cross sections for reaction (2) were taken from Straub *et al.*[13] In their experiment, a time-of-flight mass spectrometer was used to distinct charged particles according to their mass-to-charge ratios. For this reason, N^+

* 1 eV = 1.602×10^{-19} J

generated in the dissociative ionization process were detected together with N_2^{2+}, that can also be created by electron impact. However, N_2^{2+} can practically be produced only in trace amounts under the considered conditions, because the highest electron energies within this work were approximately 60 eV, while the threshold for the second ionization energy of N_2 is 42.88 eV.[9] The high-energy tail of the EEDF barely crosses the threshold for the second ionization energy of N_2 (even under conditions for which the highest energies are achieved) and very small amount of electrons are capable of performing the second ionization of the N_2 molecule. Therefore, it was consider appropriate to refer to the cross sections of Straub *et al.* as the cross sections for dissociative ionization within this work.[13] These cross sections were supplemented by including the threshold value for dissociative ionization of 24.29 eV.[9] The cross-section values between the threshold and the first electron energy reported by Straub *et al.*,[13] which was 30 eV, were linearly interpolated. The integral cross sections used for reactions (1) and (2) in the present manuscript are shown in Fig. 1.

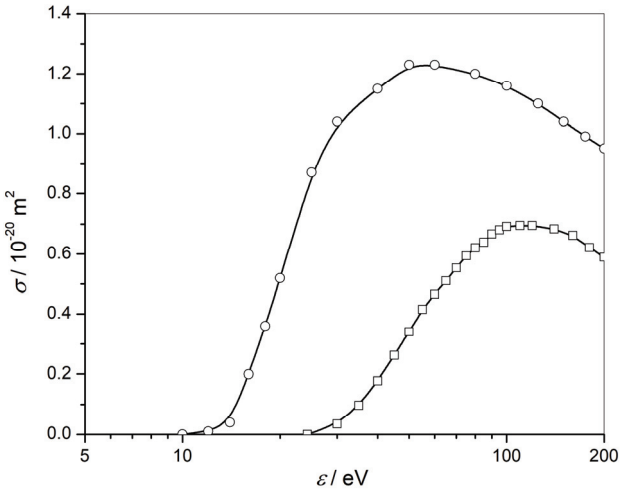

Fig. 1. Integral cross sections for the dissociation of N_2 to neutral fragments of Cosby[10] (circles) and for dissociative ionization of Straub *et al.*[13] (squares) *vs*. electron energy.

METHOD

Monte Carlo simulation

In order to simulate the motion of electrons through the N_2 gas under the presence of time-varying electric and magnetic fields, the Monte Carlo (MC) code used in earlier works of our group,[14,15] was modified and used.[16] The motion of the electron is described by the following differential equation:

$$m\frac{\mathrm{d}^2\mathbf{r}}{\mathrm{d}t^2} = e\left(\mathbf{E}(t) + \frac{\mathrm{d}\mathbf{r}}{\mathrm{d}t}\mathbf{B}(t)\right) \tag{3}$$

In Eq. (3), **r** is the radius vector of the electron, *m* and *e* are the mass and charge of the electron, **E** and **B** are the electric and magnetic field vectors, respectively, and *t* is time. The time-varying electric and magnetic field vectors periodically oscillate at fixed frequency are described by Eqs. (4) and (5):

$$\mathbf{E}(t) = \sqrt{2}E_{\mathrm{R}}\cos(2\pi ft)\mathbf{k} \quad (4)$$

$$\mathbf{B}(t) = \sqrt{2}B_{\mathrm{R}}\sin(2\pi ft)\mathbf{j} \quad (5)$$

where **k** and **j** are the unit vectors in the Cartesian coordinate system that characterize the direction of electric and magnetic fields, while *f* is the frequency of their oscillation. E_{R} and B_{R} are the root mean square values of the electric and magnetic field, respectively. Absolute values of electric and magnetic field within this work will be replaced with reduced electric field and reduced magnetic field, defined as quotients E_{R}/N and B_{R}/N, *N* being the gas number density. The electric and magnetic fields are mutually perpendicular, and phase shift among them is $\pi/2$ rad. The numerical solutions of the Eq. (3) were used to calculate the position and velocity of the electron in each small time step of the simulation (much smaller than the period of oscillation) by the numerical iterative Runge–Kutta method.[17]

Electrons were generated with a certain value of the kinetic energy and were simulated one by one under the defined conditions (E_{R}/N, B_{R}/N and *f* values specified). The simulation procedures follow every electron until it reaches the quasi-steady state, *i.e.*, the state where energy received from the electric field is balanced with the energy that is lost in non-elastic collisions with the N_2 molecules. When the quasi-steady state was reached, the ensemble of electrons obtains stable oscillations of mean electrons energy (ε_{m}) over time and at this point the EEDFs were sampled over one period of the fields oscillation. These EEDFs are essential for obtaining the rate coefficients, as shall be explained further.

The nitrogen gas in which the electrons were simulated was considered to be at 133.3 Pa ($N = 3.22\times10^{22}$ m^{-3}) and the zero-temperature gas approximation was used, meaning that every N_2 molecule was in its ground electronic, vibrational and rotational state. The procedures of the simulation included the possibilities of all real electron-molecule interactions under the conditions assumed: elastic collisions, non-elastic collisions (rotational, vibrational and electronic excitations) as well as ionization. The database of the simulations containing the cross sections for all relevant processes was carefully composed. The probability of a certain scattering process at a given electron energy ε depended on the corresponding effective cross section $\sigma(\varepsilon)$. The decision as to which collision process will occur was left to a pseudo-random generated number, as were the scattering angles of the electron after the collision. Electrons that were created in the ionization process were also simulated. The MC code was successfully tested on model gases,[18,19] by comparing the transport parameters of the electrons with the benchmark values from the literature.[20] For other details about the MC code, see Ristić *et al.* and Ristić *et al.*[15,16]

Cross-section database

Finding an optimal set of cross-sections for the electron-N_2 molecule interaction was crucial for a successful simulation. For elastic scattering, the recent cross-section data of Allan in the electron energy range from 0 to 5.5 eV was used.[21] For electron energies from 6 to 10 eV, the data of Sun *et al.* was used,[22] while in the energy region from 10 to 70 eV, the data of Gote and Ehrhardt was used.[23] In the high-energy region from 70 to 90 eV, the data of Nickel *et al*.[24] was used.

Cross-section values for rotational excitations were adopted from Itikawa and Mason for $J = 0 \rightarrow 2$ and $J = 0 \rightarrow 4$ excitations.[25] For vibrational excitations, the integral cross-sections

that were measured in our laboratory were used.[26] These measurements include excitations into the first ten vibrational levels of the ground electronic state of the N_2 molecule.

The cross-sections for $a'^1\Sigma_u^-$, $w^1\Delta_u$ and $a''^1\Sigma_g^+$ singlet electronic states were adopted from Itikawa,[27] compilation proposed by Brunger *et al*.,[28] based on the experiments of Trajmar *et al.* and Campbell *et al*.,[29,30] and the theoretical calculations of Ohmori *et al.* and Gillan *et al.*[31,32] The cross-section values were also taken from Brunger *et al*,[28] for the excitation of $a^1\Pi_g$ state on the basis of electron energy loss measurements of Finn and Doering,[33] direct detection of the excited molecule of Mason and Newell and swarm experiments.[34,35] For the $c_4'^1\Sigma_u^+$ and $b'^1\Sigma_u^+$ states, values from Ajello *et al.* were taken.[35] The $b^1\Pi_u$ state cross-section was adopted from James *et al.*,[36] and recent cross-section measurements of the $c_3^1\Pi_u$ and $o_3^1\Pi_u$ states were adopted from Malone *et al*.[37] The values of the cross sections for the excitations of the $A^3\Sigma_u^+$, $B^3\Pi_g$, $W^3\Delta_u$ and $B'^3\Sigma_u^-$ triplet electronic states were used from Itikawa,[27] which were recommended by Brunger *et al.* based on previously mentioned studies.[28-32] Cross-section proposed by Brunger *et al.*,[28] for $E^3\Sigma_g^+$ state (based on several beam experiments)[29,30,38,39] and for $C^3\Pi_u$ state (based also on beam experiments)[29,30,39,40] were used. $F^3\Pi_u$ and $G^3\Pi_u$ electronic state cross sections were used from Malone *et al.*[37] Ionization cross sections were adopted from Itikawa,[27] based on Lindsay and Mangan[41] and Straub *et al.* measurements.[13] Dissociation was included implicitly by taking into account all significant electronic states that contribute to it, as was explained in the Introduction section.

Validation of the present cross-section database for nitrogen was performed by comparing basic transport properties of electrons (drift velocities and diffusion coefficients) obtained by the present simulation with the experimentally measured ones. In a previous works we presented these comparisons for drift velocity, longitudinal diffusion coefficient and ionization coefficient, whereby excellent agreements were obtained.[14,42] Comparison was also made with the Boltzmann equation-based software BOLSIG+ (version 1.1).[43] By including the present cross-section database in both our Monte Carlo simulation and BOLSIG+ oscillating field routine, we obtained the agreement of period averaged mean electron energy within 2 % only.

Rate coefficient calculation

The EEDFs and corresponding mean electron energies were sampled within one phase of the electric field oscillation after the quasi-steady state was reached in the simulation. The EEDFs obtained were then normalized by the relation:

$$\int_0^\infty f_\varepsilon(\varepsilon_m,\varepsilon,t)\,\mathrm{d}\varepsilon = 1 \tag{6}$$

In Eq. (6), the normalized EEDF at the specific time t is denoted by $f_\varepsilon(\varepsilon_m, \varepsilon, t)$, while ε represents the actual kinetic energy of the electron. For every $f_\varepsilon(\varepsilon_m,\varepsilon,t)$ in the specific moment in time (that is, in the specific phase of the electric field oscillation), the corresponding rate coefficient, $k(\varepsilon_m, t)$ was calculated by the following relation:[44]

$$k(\varepsilon_m,t) = \sqrt{\frac{2}{m}}\int_{\varepsilon_{th}}^\infty \sigma(\varepsilon)\sqrt{\varepsilon} f_\varepsilon(\varepsilon_m,\varepsilon,t)\,\mathrm{d}\varepsilon \tag{7}$$

where $\sigma(\varepsilon)$ is the effective cross-section for a given process with a threshold energy ε_{th}.

RESULTS AND DISCUSSION

According to Eq. (7), the rate coefficients for dissociation processes (1) and (2) were calculated by implementing the EEDFs obtained after reaching the quasi-steady state by the MC code for given input parameters. The input parameters imply E_R/N values of 300 and 500 Td (1 Td = 10^{-21} V m^2), B_R/N values

of 0, 1000 and 2000 Hx (1 Hx = 10^{-27} T m^3) and values of frequency 13.56, 100 and 200 MHz. As stated earlier, the integral cross sections for the calculation of the rate coefficients for the dissociation of N_2 to neutral fragments were adopted from Cosby,[10] while the rates for dissociative ionization were calculated based on integral cross sections measured by Straub *et al.* with implemented energy threshold for process (2).[9,13] Background physics of electrons motion in crossed electric and magnetic RF fields is well known and will only be slightly addressed in this paper.[16,20]

Since the MC simulation records many EEDFs within one period of the field's oscillation, a fine time evolution of the rate coefficients on the nanosecond scale was obtained. The rate coefficients for dissociation of N_2 to neutral fragments are presented on Fig. 2. for all input parameters. First, it should be noticed that the rate coefficients are oscillating at twice the frequency of the applied RF fields. The reason is that the energy of the electron is independent of the absolute direction of the electric field. The rate coefficients depend on all the varied parameters. It should be noted that when discussing the dependence of the rate coefficient on one specific parameter, the other parameters are considered as constant.

By observing the coefficients at the lowest considered frequency of 13.56 MHz for given E_R/N and B_R/N, it was noticeable that the highest and lowest (zero) amplitude values of the coefficients were reached, which is expected because at that frequency, the electrons efficiently track the electric field changes and lag only slightly behind them. Therefore, when the electric field (which determines the energy of the electron) reaches a maximum or minimum, the EEDF also has the largest share of high-energy electrons (for given E_R/N and B_R/N) and consequently, the rate coefficient is the largest. On the other hand, when the electric field passes through the zero value, after which the electrons are slowed down, the share of fast electrons in the EEDF is the smallest and the rate coefficient reaches its lowest value. At 13.56 MHz, this lowest value is zero, as can be seen from Fig. 2.

At higher frequencies, the EEDFs have a narrowed oscillation range due to a more pronounced electron delay behind the electric field. For this reason, the rates also oscillate over a narrower range: they do not reach the maximum amplitude values they had at lower frequencies, but they do not fall to zero either. One of the characteristics of the time evolution of the rate coefficients is the existence of phase delay with respect to the electric field. This delay is also a consequence of the inertia of the motion of electrons through the N_2 gas and is more pronounced at higher frequencies.[14]

Regarding the influence of the strength of the electric and magnetic fields on the appearance of the rate coefficients, they are also noticeable in Fig. 2. Both electric and magnetic field strongly affect the value of the rates. At stronger electric fields, the share of high-energy tail of EEDF is higher, and thus the overlap

integral in Eq. (7) is higher, which leads to a higher values of the rate coefficients.

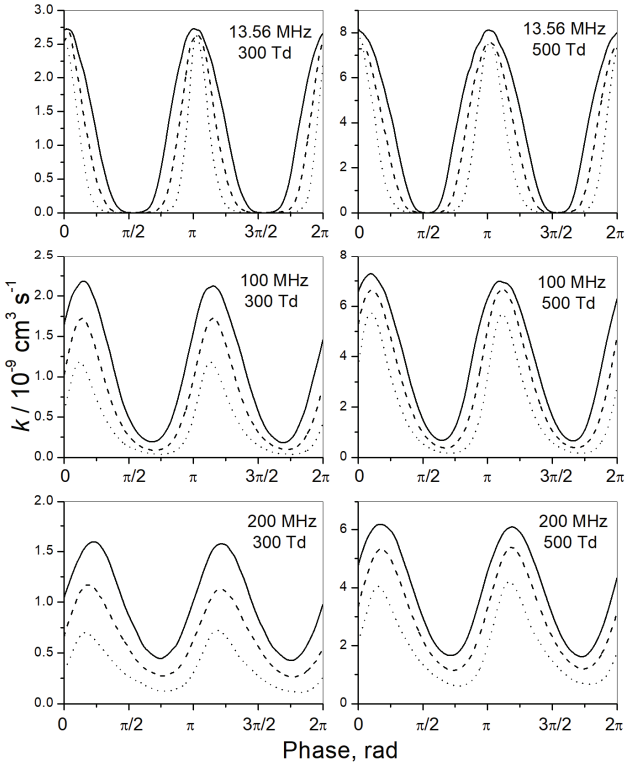

Fig. 2. Rate coefficients for the dissociation of N_2 to neutral fragments *vs.* the phase of the RF electric field at the indicated pair of f and E_R/N and for $B_R/N = 0$ Hx (full line), $B_R/N = 1000$ Hx (dashed line) and $B_R/N = 2000$ Hx (dotted line).

At higher B_R/N values, the profile of the rate coefficient with time is narrowed and at the same time reduced in height, due to the complex action of the magnetic field on the electrons. Hence the overall effect of increasing magnetic field on the rate coefficients shown here is their reduction.

For most practical applications in which nitrogen dissociation may be of interest in plasma chemistry and plasma technology of nitrogen-containing systems, an important fact is the time-averaged rate coefficient during one period of RF field oscillation. To this end, these period averaged rates for the dissociation of N_2 into neutral fragments are given Table I for all considered parameters. In the ranges of varied input parameters, the average rate coefficient changed its value from 0.341×10^{-9} to 3.929×10^{-9} cm^3 s^{-1}. By analyzing the data in Table I, it could be concluded that an increase of E_R/N leads to larger values of the rate coefficient, while an increase of B_R/N leads to their lowering. Increasing the fre-

quency does not have much effect on the value of the period averaged rate coefficients, nor can its effect be easily generalized.

TABLE I. Period averaged rates (10^{-9} cm^3 s^{-1}) for the dissociation of N_2 into neutral fragments under various conditions

f / MHz	E_R/N = 300 Td			E_R/N = 500 Td		
	(B_R/N) / Hx					
	0	1000	2000	0	1000	2000
13.56	1.156	0.786	0.492	3.929	2.828	1.972
100	1.064	0.693	0.391	3.778	2.871	1.926
200	0.971	0.641	0.341	3.796	2.948	1.923

The rate coefficients for dissociative ionization of N_2 are presented in Fig. 3. for all input parameters. Most of what has been said about the rate coefficients of dissociation into neutral fragments also applies here: E_R/N, B_R/N and f values

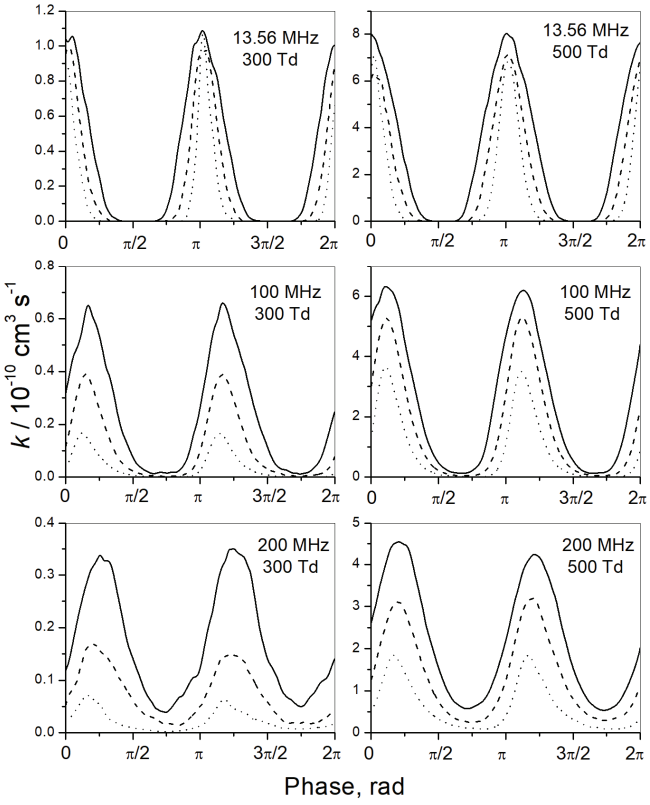

Fig. 3. Rate coefficients for dissociative ionization of N_2 *vs*. phase of the RF electric field at the indicated pair of f and E_R/N and for B_R/N = 0 Hx (full line), B_R/N = 1000 Hx (dashed line) and B_R/N = 2000 Hx (dotted line).

have qualitatively the same effect on the shape of the rates. The period averaged rates of the dissociative ionization for all considered parameters are given in Table II. However, in the case of dissociative ionization (unlike the previous case), the effect of frequency on the rates is evident. Raising the *f* significantly lowers the rate coefficients for dissociative ionization.

The rates for dissociative ionization were about 10 to 15 times lower than those for the dissociation into neutral fragments. This was expected since the cross-section for dissociative ionization is lower, while the energy threshold is higher. From Table II, it could be seen that the rate values ranged from 0.022×10^{-10} to 3.020×10^{-10} cm^3 s^{-1}. Nevertheless, dissociative ionization remains an important source of N^+ in plasmas, in addition to direct ionization of the N atom.

TABLE II. Period averaged rates (10^{-10} cm^3 s^{-1}) for dissociative ionization under various conditions

f / MHz	E_R/N = 300 Td			E_R/N = 500 Td		
	(B_R/N) / Hx					
	0	1000	2000	0	1000	2000
13.56	0.3493	0.2153	0.1275	3.020	1.939	1.271
100	0.2364	0.1112	0.0391	2.494	1.614	0.858
200	0.1699	0.0713	0.0225	2.181	1.309	0.604

Recently, Sode *et al.* developed a new model for the calculation of ion and radical densities in inductively coupled nitrogen plasmas.[45] They proposed the equations for the calculation rate coefficients for numerous elementary processes in plasma, among them the dissociation of N_2 to neutral fragments and for the dissociative ionization of N_2 (see Table II of their work, reactions 1.6 and 1.9). By implementing the mean electron energy obtained from the present MC simulation in their equations, significant difference in the values of the rate coefficients were obtained.

For example, at 13.56 MHz, 300 Td and 0 Hx, the mean electron energy obtained by the present MC code was 6.47 eV and the rate for dissociation to neutral fragments was 3.6×10^{-9} cm^3 s^{-1} (the present value was 1.1×10^{-9} cm^3 s^{-1}), while for dissociative ionization, the rate was 1.1×10^{-10} cm^3 s^{-1} (the present value was 0.35×10^{-10} cm^3 s^{-1}). Sode *et al.* stated that they assumed Maxwellian EEDF in their equations,[45] but here it could be seen that the dissociation rates in that case were roughly three times higher than the ones presented here, based on non-equilibrium EEDFs. In addition, the rates obtained in that way were independent of the magnetic field or frequency values. Note that the cross sections that Sode *et al.* used were practically the same as those used here. The described example shows that the dissociation coefficients presented here could significantly improve the kinetic calculations in nitrogen plasma chemistry.

CONCLUSIONS

The rate coefficients for electron impact dissociation of the N_2 molecule to neutral fragments, as well as for the dissociative ionization process were calculated under the presence of RF electric and magnetic fields. The choice of parameters included three frequencies: 13.56, 100 and 200 MHz, two E_R/N values: 300 and 500 Td and B_R/N values: 0, 1000 and 2000 Hx.

Therefore, the nitrogen molecule dissociation processes, as one of the most important processes in nitrogenous RF plasma chemistry, were quantified for the stated conditions. Fine temporal evolution of the dissociation rate coefficients within the RF field phase was presented with an adequate explanation. The time-averaged values of the rate coefficients were also shown. Dissociative ionization is by an order of magnitude a rarer process compared to dissociation into neutral fragments, which is expected due to its lower cross-section values and higher threshold.

Acknowledgements. This work was supported in part by the Ministry of Education, Science and Technological Development of the Republic of Serbia under contracts No. 451-03-68/2022-14/200146 and 451-03-9/2022-14/200162. The authors gratefully acknowledge the assistance of Muna Aoneas.

И З В О Д

ДИСОЦИЈАЦИЈА N_2 УДАРОМ ЕЛЕКТРОНА У ЕЛЕКТРОМАГНЕТНИМ RF ПОЉИМА

МИРОСЛАВ РИСТИЋ[1], РАДОМИР РАНКОВИЋ[1], МИРЈАНА М. ВОЈНОВИЋ[2], ВИОЛЕТА В. СТАНКОВИЋ[2] и ГОРАН Б. ПОПАРИЋ[2]

[1]*Универзитет у Београду – Факултет за физичку хемију, Студентски трг 12-16, Београд и* [2]*Универзитет у Београду – Физички факултет, Студентски трг 16, Београд*

Коефицијенти брзине дисоцијације молекула N2 ударом електрона под утицајем укрштеног радиофреквентног (RF) електричног и магнетног поља израчунати су за фреквенције од 13.56, 100 и 200 MHz и за средње квадратне вредности редукованог електричног поља од 300 и 500 Td. Средње квадратне вредности редукованог магнетног поља вариране су од 0 до 2000 Hx. Дискутовани су ефекти јачина RF поља и њихове фреквенције на коефицијенте брзине за дисоцијацију на неутралне фрагменте и за дисоцијативну јонизацију. Приказана је и продискутована временска еволуција коефицијената брзине у току једног периода RF поља.

(Примљено. 10. јула, ревидирано 5. августа, прихваћено 8. августа 2022)

REFERENCES

1. E. Guiberteau E, G. Bonhomme, R. Hugon, G. Henrion, *Surf. Coat. Technol.* **97** (1997) 552 (https://doi.org/10.1016/S0257-8972(97)00188-6)
2. D. D. Markushev, J. Jovanović-Kurepa, M. Terzić, *Rev. Sci. Instrum.* **74** (2003) 303 (https://doi.org/10.1063/1.1515900)
3. C. Zhang, L. Fu, N. Liu, M. Liu, Y. Wang, Z. Liu, *Adv. Mater.* **23** (2011) 1020 (https://doi.org/10.1002/adma.201004110)

4. S. Villeger, J. P. Sarrette, B. Rouffet, S. Cousty, A. Ricard, *Eur. Phys. J. Appl. Phys.* **42** (2008) 25 (http://dx.doi.org/10.1051/epjap:2007177)
5. A. S. Dobrota, I. A. Pašti, S. V. Mentus, B. Johansson, N. V. Skorodumova, *Appl. Surf. Sci.* **514** (2020) 145937 (https://doi.org/10.1016/j.apsusc.2020.145937)
6. E. C. Zipf, R.W. McLaughlin, *Planet. Space Sci.* **26** (1978) 449 (https://doi.org/10.1016/0032-0633(78)90066-1)
7. A. E. S. Green, C. A. Barth, *J. Geophys. Res.* **72** (1967) 3975 (https://doi.org/10.1029/JZ072i015p03975)
8. N. Itagaki, S. Iwata, K. Muta, A. Yonesu, S. Kawakami, N. Ishii, Y. Kawai, *Thin Solid Films* **435** (2003) 259 (https://doi.org/10.1016/S0040-6090(03)00395-X)
9. O. Dutuit, N. Carrasco, R. Thissen, V. Vuitton, C. Alcaraz, P. Pernot, N. Balucani, P. Casavecchia, A. Canosa, S. L. Picard, J. Loison, Z. Herman, J. Zabka, D. Ascenzi, P. Tosi, P. Franceschi, S. D. Price, P. Lavvas, *Astrophys. J. Suppl. Ser.* **204** (2013) 45 (https://doi.org/10.1088/0067-0049/204/2/20)
10. P. C. Cosby, *J. Chem. Phys.* **98** (1993) 9544 (https://doi.org/10.1063/1.464385)
11. H. F. Winters, *J. Chem. Phys.* **44** (1966) 1472 (https://doi.org/10.1063/1.1726879)
12. Y. Itikawa, *J. Phys. Chem. Ref. Data* **35** (2006) 31 (https://doi.org/10.1063/1.1937426)
13. H. C. Straub, P. Renault, B. G. Lindsay, K. A. Smith, R. F. Stebbings, *Phys. Rev., A* **54** (1996) 2146 (https://doi.org/10.1103/PhysRevA.54.2146)
14. M. P. Popović, M. M. Vojnović, M. M. Aoneas, M. Ristić, M. M. Vićić, G. B. Poparić, *Phys. Plasmas* **21** (2014) 063504 (https://doi.org/10.1063/1.4975312)
15. M. M. Ristić, M. Aoneas, M. M. Vojnović, G. B. Poparić, *Plasma Chem. Plasma Process.* **37** (2017) 1431 (https://doi.org/10.1007/s11090-017-9826-6)
16. M. M. Ristić, V. V. Stanković, M. M. Vojnović, G. B. Poparić, *Phys. Plasmas* **29** (2022) 093514 (https://doi.org/10.1063/5.0101931)
17. R. Morrow, *J. Comput. Phys*. **43** (1981) 1 (https://doi.org/10.1016/0021-9991(81)90108-X)
18. K. Maeda, T. Makabe, N. Nakano, S. Bzenić, Z. Lj. Petrović, *Phys. Rev., E* **55** (1997) 5901 (https://doi.org/10.1103/PhysRevE.55.5901)
19. H. T. Saelee, J. Lucas, *J. Phys., D* **8** (1975) 640 (https://doi.org/10.1088/0022-3727/10/3/014)
20. Z. Lj. Petrović, Z.M. Raspopović, S. Dujko, T. Makabe, *Appl. Surf. Sci.* **192** (2002) 1 (https://doi.org/10.1016/S0169-4332(02)00018-1)
21. M. Allan, *J. Phys., B* **38** (2005) 3655 (https://doi.org/10.1088/0953-4075/38/20/003)
22. W. Sun, M. A. Morrison, W. A. Isaacs, W. K. Trail WK, D. T. Alle, R. J. Gulley, M. J. Brennan, S. J. Buckman, *Phys. Rev., A* **52** (1995) 1229 (https://doi.org/10.1103/PhysRevA.52.1229)
23. M. Gote, H. Ehrhardt, *J. Phys., B* **28** (1995) 3957 (https://doi.org/10.1088/0953-4075/28/17/029)
24. J. C. Nickel, C. Mott, I. Kanik, D. C. McCollum, *J. Phys., B* **21** (1988) 1867 (https://doi.org/10.1088/0953-4075/21/10/018)
25. Y. Itikawa, N. Mason, *Phys. Rep.* **414** (2005) 1 (https://doi.org/10.1016/j.physrep.2005.04.002)
26. M. Ristić, G. B. Poparić, D. S. Belić, *Chem. Phys.* **331** (2007) 410 (https://doi.org/10.1016/j.chemphys.2006.11.012)
27. Y. Itikawa, *Phys. Chem. Ref. Data* **35** (2006) 31 (https://doi.org/10.1063/1.1937426)

28. M. J. Brunger, S. J. Buckman, M. T. Elford, *Photon and electron interactions with atoms, molecules and ions*, Springer, New York, 2003 (https://doi.org/10.1007/b83711)
29. S. Trajmar, D. F. Register, A. Chutjian *Phys. Rep.* **97** (1983) 219 (https://doi.org/10.1016/0370-1573(83)90071-6)
30. L. Campbell, M. J. Brunger, A. M. Nolan, L. J. Kelly, A. B. Wedding, J. Harrison, P. J. O. Teubner, D. C. Cartwright, B. McLaughlin, *J. Phys., B* **34** (2001) 1185 (https://doi.org/10.1088/0953-4075/34/7/303)
31. Y. Ohmori, M. Shimozuma, H. Tagashira, *J. Phys., D* **21** (1988) 724 (https://doi.org/10.1088/0022-3727/21/5/009)
32. C. J. Gillan, J. Tennyson, B. M. McLaughlin, P. G. Burke, *J. Phys., B* **29** (1996) 1531 (https://doi.org/10.1088/0953-4075/29/8/017)
33. T. G. Finn, J. P. Doering, *J. Chem. Phys.* **64** (1976) 4490 (https://doi.org/10.1063/1.432075)
34. N. J. Mason, W. R. Newell, *J. Phys., B* **20** (1987) 3913 (https://doi.org/10.1088/0022-3700/20/15/035)
35. J. M. Ajello, G. K. James, B. O. Franklin, D. E. Shemansky, *Phys. Rev., A* **40** (1989) 3524 (https://doi.org/10.1103/PhysRevA.40.3524)
36. G. K. James, J. M. Ajello, B. Franklin, D. E. Shemansky, *J. Phys., B* **23** (1990) 2055 (https://doi.org/10.1088/0953-4075/23/12/015)
37. C. P. Malone, P. V. Johnson, X. Liu, B. Ajdari, I. Kanik, M. A. Khakoo, *Phys. Rev., A* **85** (2012) 062704 (https://doi.org/10.1103/PhysRevA.85.062704)
38. M. J. Brunger, P. J. O. Teubner, S. J. Buckman, *Phys. Rev., A* **37** (1988) 3570 (https://doi.org/10.1103/PhysRevA.37.3570)
39. M. Zubek, G. C. King, *J. Phys., B* **27** (1994) 2613 (https://doi.org/10.1088/0953-4075/27/12/019)
40. G. Poparić, M. Vićić, D. S. Belić, *Chem. Phys.* **240** (1999) 283 (https://doi.org/10.1016/S0301-0104(98)00383-8)
41. B. G. Lindsay, M. A. Mangan, *Photon and electron interactions with atoms, molecules and ions. Interactions of photons and electrons with molecules*, Springer, New York, 2003 (https://doi.org/10.1007/b83711)
42. M. Vojnović, M. Popović, M. M. Ristić, M. D. Vićić, G. B. Poparić, *Chem. Phys.* **463** (2015) 38 (https://doi.org/10.1016/j.chemphys.2015.09.014)
43. G. J. M. Hagelaar, L. C. Pitchford, *Plasma Sources Sci. Technol.* **14** (2005) 722 (https://doi.org/10.1088/0963-0252/14/4/011)
44. D. S. Belić, *Chem. Phys.* **130** (1989) 141 (https://doi.org/10.1016/0301-0104(89)87043-0)
45. M. Sode, W. Jacob, T. Schwarz-Selinger, H. Kersten, *J. Appl. Phys.* **117** (2015) 083303 (http://dx.doi.org/10.1063/1.4913623).